



OPEN Involvement of tdTomato-Tagged RPE cells in a mouse PVR model with enzymatically compromised retina

Yao Chen^{1,2,6}, Xiao Liu^{1,3,6}, Ashwini Kini¹, John Y. Liu^{1,4}, Xiaoqin Lu^{1,4}, Ling Gao³, Henry J. Kaplan^{1,5}, Douglas C. Dean^{1,4}✉ & Yongqing Liu^{1,4}✉

Ocular trauma and surgery are considered the most common cause for proliferative vitreoretinopathy (PVR). Many retinal cell types are thought to be the cellular source for PVR although most risk factors for PVR are associated with intravitreal dispersion of the retinal pigment epithelium (RPE) cells. Major PVR animal models are rabbit and swine with an artificial implantation of exogenous cells into the vitreous to form epiretinal membrane (ERM) which does not recapitulate a real PVR pathology. To clarify and validate the participation of RPE cells, to mimic ocular trauma in situ, and to reveal the related macromolecule changes in PVR pathology, we utilized a dispase treatment to damage the retina in establishment of a reliable RPE-tagged PVR mouse model with ERM-like tissues formed within and on both surface of the retina. The immunostaining of patient epiretinal membranes with lineage markers confirms RPE is involved in PVR development. Quantitative PCR analysis indicates the dedifferentiation of RPE cells switches RPE from epithelial to mesenchymal phenotype to re-enter a proliferative and mobile state underlying PVR. Gene expression results of the mouse PVR model retinas are consistent with the microarray gene expression profile of human PVR retinas, validating that our mouse PVR model resembles human PVR and is thereby suitable for molecular mechanism and pharmaceutical studies.

Keywords Proliferative vitreoretinopathy, Retinal pigment epithelium, Epiretinal membrane, PVR mouse model, RPE cell migration

Proliferative vitreoretinopathy (PVR) occurs in approximately 5–10% retinal detachment cases and remains the most common cause of failure for surgical intervention of retinal detachment^{1,2}, leading to recurrent retinal detachment; but the pathophysiology underlying PVR is not fully understood³. The cause of PVR is the damage of the retina including retinal tears, eye trauma or surgeries, choroidal detachment, so that ectopic cells can opportunistically situate in and/or on the retina⁴. According to the clinical observation, these cells secrete matrix proteins to form fibrotic membranes/bands on/in the retina⁵. As abnormal cell proliferation and fibrotic tissue formation are the major pathological features of PVR, inhibiting the ectopic cell growth and impeding potential fibrosis-related molecular pathways are considered the therapeutic solutions to prevent PVR^{6,7}. PVR epiretinal membrane (ERM) formation is a complicated process possibly involving various cell types and inflammation-inducible factors. The ERM either surgically removed from patients or harvested from animal PVR experimental models are mainly composed of myofibroblasts with the origin of the RPE, Müller and microglial cells, that produce a large quantity of smooth muscle actin alpha (SMA α), thereby causing retinal contraction and recurrent retinal detachment^{8–11}. Moreover, in vivo studies show that under certain circumstances, RPE, Müller and microglial cells can transdifferentiate into myofibroblasts upon an epithelial to mesenchymal transition (EMT),

¹Department of Ophthalmology and Visual Sciences, University of Louisville School of Medicine, Louisville, KY 40202, USA. ²Department of Ophthalmology, Hunan Key Laboratory of Ophthalmology, National Clinical Research Center for Geriatric Disorders, Xiangya Hospital, Central South University, Changsha 410011, Hunan Province, China. ³Department of Ophthalmology, the Second Affiliated Hospital, Central South University, Changsha 410011, Hunan Province, China. ⁴Department of Medicine, James Brown Cancer Center, University of Louisville School of Medicine, Louisville, KY 40202, USA. ⁵Department of Ophthalmology, St. Louis University School of Medicine, St. Louis, MO 63110, USA. ⁶Yao Chen and Xiao Liu contributed equally. ✉email: dcdean01@louisville.edu; yoliu016@louisville.edu

enabling cell migration, invasiveness, resistance to apoptosis and secretion of large quantity of extracellular matrix (ECM)^{11–13}.

RPE cells are considered as a key source in pathogenesis of PVR mainly because of their capability to proliferate, to migrate and to produce fibrotic tissues such as the ERM⁸, although their participation in ERM formation of non-rhegmatogenous retinal detachment remains debatable, as no conceivable cleavage can be found in diseases such as idiopathic retinal membrane¹⁴. Yet, how RPE cells are detached from the quiescent RPE layer and migrate to the epiretinal surface are not fully clarified. Furthermore, RPE cells are difficult to trace because their specific cell markers like RPE65 are likely to lose after the EMT¹². In contrast, the myofibroblast-like RPE cells would express SMA α , vimentin and even microglial cell marker GFAP in the ERM⁸. The expression of multiple markers makes it more difficult to identify the cellular origin of the ERM. In order to make sure RPE origin, several animal models injected RPE cells into the vitreous to artificially create PVR^{15–17}. In these models, RPE cells have been proved to undergo EMT and to possess myofibroblast-like features thereby facilitating the formation of the PVR-like retinal membranes¹⁸. However, the grafted RPE cells are heterologous to the host, which in fact do not represent the natural PVR formation in human eyes and spark a host immune rejection response that is not present in PVR pathology. In tracing RPE functionality and activity during PVR development without intravitreally injecting exogenous RPE cells, we developed an RPE-tagged mouse PVR model in which the RPE cells constantly and specifically express the red fluorophore tdTomato. Compared to the human ERMs and PVR retinas, our mouse PVR model likely recapitulates most features of human PVR, providing a straightforward and reliable method in studying roles of RPE cells in PVR development and their underlying molecular mechanisms.

Methods

Ethics statement

This study was approved by the Institutional Review Board of University of Louisville and adhered to the tenets of the Declaration of Helsinki. Adult human eyes were obtained from the eye bank of Kentucky Lions Eye Center at Louisville. The epiretinal membrane (ERM) samples were collected at the time of surgeries. Written informed consent was obtained. The ERM samples were stored in PBS at -80°C and processed to be fixed in 4% paraformaldehyde (PFA) and then immunostaining with desired antibodies. Animal surgery procedures were approved by the Institutional Animal Care and Use Committee (IACUC) of the University of Louisville. All animal experiments were conducted in accordance with the guidelines of Association for Research in Vision and Ophthalmology (ARVO) and the Animal Research Reporting of In Vivo Experiments (ARRIVE) on the use of animals in research.

Animals

C57BL/6.Cg-Gt(ROSA26Sortm14(CAG-tdTomato)Hze>/J mice (CAG-STOP^{flf}-tdTomato, Jackson Laboratory, stock #: 007914) harbor a targeted mutation of the Gt(ROSA)26Sor locus with a loxP-flanked STOP cassette (STOP^{flf}) preventing transcription of the CAG promoter-driven red fluorescent protein variant tdTomato. The CAG promoter is a strong synthetic promoter frequently used to drive high levels of gene expression in mammalian cells. C57BL/6-Tg(BEST1-cre)1Jdun/J (BEST1-Cre, Jackson Laboratory stock #: 017557) mice express the Cre recombinase under the control of human bestrophin 1 (BEST1) gene promoter. BEST1 gene is specifically expressed in RPE cells. We crossbred CAG-STOP^{flf}-tdTomato mice with BEST1-Cre mice to generate RPE lineage tracer CAG-tdTomato mice where the red Fluorescence tdTomato was constantly expressed in the RPE following Cre-mediated recombination. All C57BL/6 and BALB/c mice were inbred in the animal facility of the University of Louisville.

Mouse PVR induction and therapeutical treatment

Eight-week-old mice with C57BL/6 background and BALB/c of both sexes were anesthetized by an intraperitoneal (IP) injection of 100 mg/kg ketamine and 5 mg/kg xylazine. Four methods were used to induce PVR: (1) 23 mice were intravitreally injected 3 μL of 0.6 U/mL dispase (Roche Diagnostics cat. #: 295 825) in PBS in one eye and 3 μL of PBS as a sham control in the other eye; (2) 11 mice with one retina carefully scrapped (or so-called “massage”) 5–10 times with a 34G blunt needle until bleeding was seen to physically compromise its histological structure and the other retina not scrapped by the needle as a sham control; (3) 28 mice with one eye treated with the dispase and the physical massage and the other eye served as a PBS sham control; (4) 9 mice with one eye treated with the dispase and the physical massage plus 0.3 μM dasatinib as reported¹⁹ and the other eye served as a PBS sham control. The concentration of dispase, i.e., 0.6 U/mL, was selected based on our initial test range, i.e., 0.3, 0.6, 1.2 and 2.4 U/mL, because all concentrations, except for 0.2 U/mL, resulted in more than 80% induction of PVR-like retina (data not shown). Two and seven weeks later, the treated mice were checked by two lab trained persons blinded to the mouse treatments for a possible retina tears or folds as a clinical sign of PVR formation under a Zeiss surgical microscope. All studied eyes were enucleated after euthanasia by CO_2 in a sealed container right after the last microscope examination, fixed in formalin, embedded in paraffin and sectioned at 10 μm for H&E histological staining for a microscopic retinal folding assessment, a histological sign of retinal folds and PVR formation.

Primary RPE cell isolation and culture

Mouse eyeball enucleation, RPE tissue isolation, and primary RPE cell culture were all based on the procedures previously reported²⁰. Briefly, the posterior portion of eyecups separated from the enucleated eyeballs were digested with 0.25% trypsin solution at 37°C for 5 min. The RPE sheets were scraped off the choroid into a culture dish coated with 0.1% gelatin and were then cultured in 5% CO_2 at 37°C in DMEM with 10% FBS and 1% antibiotics (Invitrogen). Monolayer-cultured primary RPE cells were passaged when confluent at 1:1 ratio.

Immunohistochemistry

Eyeball isolation, fixation and immunohistochemistry were performed as previously reported²⁰. All primary antibodies used are listed in Supplementary Table S1.

RNA extraction and real-time quantitative PCR

Four total RNA samples were prepared from 3 dispare-induced PVR-like retinas of our mouse PVR model, 3 control retinas, 2 patient epiretinal membranes (ERM) and 2 human RPE tissues using TRIzol solution (Invitrogen). SYBR green real-time quantitative PCRs (qPCR) were performed as previously reported²⁰. PCR primer sequences were generated by the web-based program “Prime3” and shown in Supplementary Table S2. The PCR amplicons were validated by size on 1.5% agarose gels.

Microarray analysis

The microarray data set on 3 human normal and 3 PVR retinas were downloaded from the NCBI database (GSE41019) and analyzed for selected genes. The raw intensity reads of all genes/spots were first log2-transformed and then normalized to the median values across genes/spots and to the values of the house keeping gene ACTB across samples following background subtraction.

Statistical analysis

Experimental data including the microarray data were analyzed and compared the PVR retinas to the control retinas, or patient ERMs to human RPE tissues by a two-tailed equal variation t-test. The rates (%) of PVR induction by dispare, massage, and their combination and after dasatinib treatment were analyzed by the chi-squared test. The significant levels were set * $p \leq 0.05$, ** $p \leq 0.01$ and *** $p \leq 0.001$.

Results

Retinal pigment epithelial (RPE) cells are the cellular component involved in proliferative vitreoretinopathy (PVR) development

Ocular trauma or surgery is the most common cause for PVR that is characterized by the growth and contraction of cellular membranes on either side of the retinal surface or in the retina (i.e., intraretinal bands)⁴. RPE, Müller and microglia cells are considered as a cellular source for PVR⁴. To validate this, we collected 14 patient epiretinal membrane (ERM) samples and checked them under a fluorescent microscope. We found 10 out of 14 samples were highly pigmented and with many DAPI-stained nuclei (Fig. 1A, B) whereas the other 4 samples were not pigmented and with very few DAPI-stained nuclei. To clarify which cell types are contained

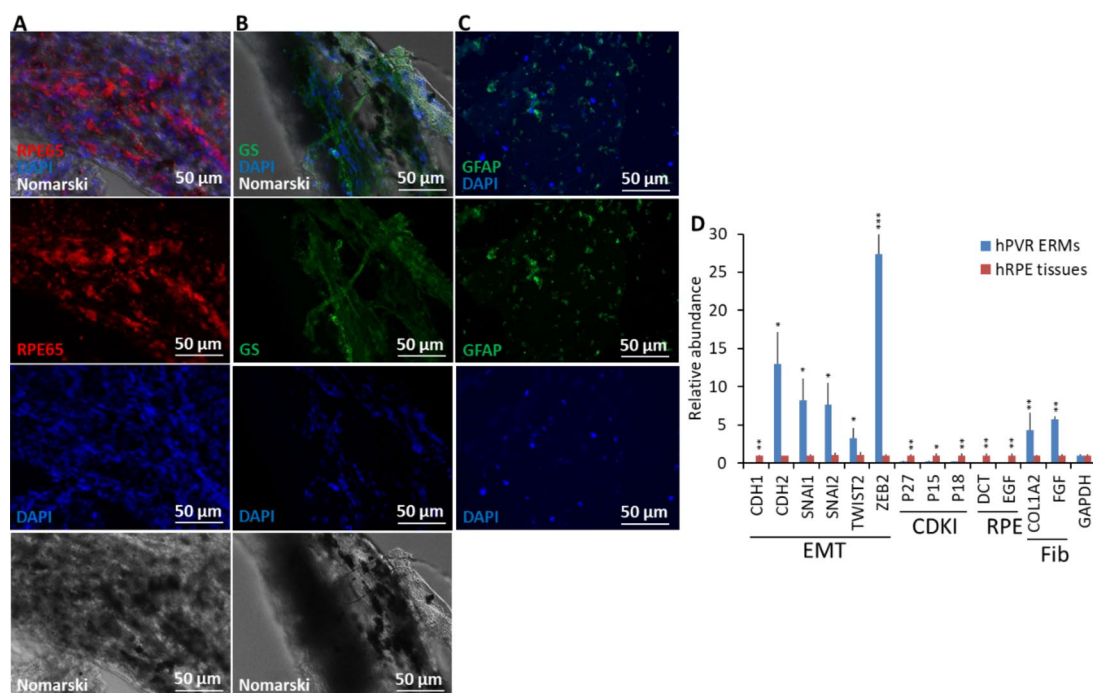


Fig. 1. Cellular and molecular analyses on patient epiretinal membrane (ERM) samples. **A** More patient ERM samples are pigmented and RPE65⁺, suggesting a RPE origin. **B** Some ERM samples are GS⁺, suggesting a Müller cell origin. **C** Some ERM samples are GFAP⁺, suggesting a microglial cell origin. **D** Three technical replicates of a mixed normal RPE tissue RNA sample from a pair of adult human eyeballs or a mixed ERM RNA sample from 2 patients were used for qPCR to detect expression of genes involving in the epithelial to mesenchymal transition (EMT), cyclin-dependent kinase inhibition (CDKI), RPE and fibroblast (Fib) cell viability. *, $p \leq 0.05$; **, $p \leq 0.01$.

in these 10 pigmented ERM samples, we immunostained them with the antibody against RPE65 for RPE cell, the GS antibody for Müller cell, and the GFAP antibody for microglial and Müller cells. As expected, most of the pigmented cells were RPE65⁺ (Fig. 1A) whereas a few of them were GS⁺ (Fig. 1B) or GFAP⁺ (Fig. 1C), suggesting the RPE cell is involved in ERM formation of PVR patients.

The separation of RPE cells from the RPE layer, the basal matrix and their neighbor cells after an ocular traumatic and/or inflammatory injury, would transdifferentiate them into a mesenchymal cell phenotype (EMT) with proliferative, mobile and fibrotic properties, which reflects the cellular characteristics of PVR. To clarify the molecular bases underlying ERM formation, we extracted total RNA from 2 patient pigmented ERMs for qPCR analysis. Compared to the normal human RPE tissue sample, the ERM sample showed loss of expression of *EGF* (a growth factor for maintaining viability of epithelial cells including RPE), *CDH1* (also known as epithelial cadherin and a common epithelial cell–cell connector), and *DCT* (an enzyme involved in RPE cell pigment synthesis) (Fig. 1D), suggesting the RPE cells in the ERMs intend to lose their original RPE epithelial properties. At the same time, the ERM cells have increased the expression of FGF (a growth factor for fibroblasts), *CDH2* (also known as neural cadherin and a common mesenchymal cell–cell connector), and *COL1A2* (a major extracellular matrix protein in the ERM) (Fig. 1D), suggesting the ERM cells have gained the properties of mesenchymal cells like fibroblasts. Loss of *CDH1* and gain of *CDH2* and a group of EMT transcription factors such as *SNAIL*, *TWIST* and *ZEB* families (Fig. 1D) are the signature for the EMT in development and tumorigenesis²¹. These molecular changes together with the loss of the expression of a group of cyclin-dependent kinase inhibitors (CDKIs) such as *P15*, *P18* and *P27* (Fig. 1D) indicate that ERM cells have regained a proliferative capacity – a critical property for PVR⁴. In addition to the presence of RPE cells in the ERMs, the high expression of both *COL1A2* and *FGF* (Fig. 1D) indicates that fibroblasts and/or myofibroblasts may also exist in the ERMs and they are likely converted from the RPE cells through EMT.

Establishment of a mouse model of PVR by an intravitreal injection of dispase

To mimic human PVR, several animal models including rodents, rabbit and swine have been created either by directly injecting exogenous cells, e.g., RPE, glia, fibroblast and macrophage, or matrix degrading enzymes, e.g., dispase and collagenase, into the vitreous, or by mechanically damaging the retina²². As PVR often occurs after an ocular trauma/surgery due to an excessive wound healing response, an artificial implantation of exogenous cells into the vitreous to form ERM does not recapitulate a real PVR pathology. To clarify which endogenous cells are truly the major cellular source to form ERM based on published literature^{23,24}, we created a mouse PVR model either by intravitreally injecting 3 μ L of 0.6U/mL dispase into 8-week-old mice or by carefully scraping (also known as “massaging”) the retina using a 35G blunt needle until the retina is bleeding (Fig. 2A) or by combining both methods, i.e., dispase together with retinal massage. Based on the clinical assessments and compared to the sham control eyes (Fig. 2B), 100% C57BL/6 mice of the dispase-treated eyes developed a PVR-like phenotype in 7 weeks (Fig. 2C–E) whereas no such PVR was discovered in the retinal “massaged” eyes (Fig. 2E), suggesting that the dispase treatment is effective to induce PVR-like phenotype in mice.

To clarify whether the retinal massage contributes to the PVR formation, we combined both the dispase and the retinal massage to damage the retina for the development of the PVR-like phenotype. It appeared that the retinal massage had a negative effect on induction of PVR as only 43% of the eyes treated by both the dispase and the retinal massage developed the PVR-like phenotype (Fig. 2E). To see whether the above results also apply to another mouse strain, we treated BALB/c mice in the same way as with the above C57BL/6 mice for developing PVR. As a result, 53% and 40% of BALB/c mice were induced to exhibit PVR-like phenotype in the eyes treated with dispase only or dispase plus massage, respectively (Fig. 2E). Again, this result validates that the dispase method is effective to induce mouse PVR-like phenotype whereas the massage has no or even negative effect on the induction of mouse PVR-like phenotype.

The small molecule dasatinib inhibits the dispase-induced mouse PVR

Dasatinib, an ATP-competitive protein tyrosine kinase inhibitor to inhibit the tyrosine kinase receptors such as BCR/Abl, Src and c-Kit, has been reported to reduce traction retinal detachment in a swine model of PVR¹⁹. To determine whether the above discovery would also apply to our mouse model of PVR we intravitreally injected 3 μ L of 0.6 U/mL dispase and 0.3 μ M dasatinib to reduce the dispase-induced mouse PVR-like phenotype. Similarly, no PVR-like phenotype was observed both clinically and histologically (Fig. 2E), suggesting the administration of dasatinib is effective to inhibit the development of the dispase-induced PVR-like phenotype in mice.

RPE lineage tracer CAG-tdTomato mice express the red fluorophore in their RPE cells both in vivo and in vitro

RPE lineage tracer CAG-tdTomato mice were generated by crossing the CAG-STOP^{fl}-tdTomato mice with the BEST1-Cre mice. In CAG-STOP^{fl}-tdTomato mice, the STOP cassette prevents the transcription of the red fluorescence *tdTomato* gene. *BEST1* gene is ubiquitously expressed in RPE cells. After crossbred with the BEST1-Cre mice, the STOP sequence in the CAG-STOP^{fl}-tdTomato cassette was removed in the RPE cells by the Cre recombinase in the hybrid pups, the CAG-tdTomato was thereby constantly expressed in the RPE cells thereafter (Fig. 3A) as CAG promoter is a strong synthetic promoter to drive high levels of gene expression in mammalian cells. To check whether the red fluorophore is specifically and efficiently tagged with the RPE cells in the adult RPE lineage tracer CAG-tdTomato mice, we enucleated their eyeballs to make cryosections. No red fluorescence was detected in their parental BEST1-Cre or CAG-STOP^{fl}-tdTomato mice, while the red fluorescence exclusively expressed along the RPE layer in all hybrid RPE lineage tracer CAG-tdTomato mice (100%) (Fig. 3B, C), suggesting that the BEST1 promoter-driven Cre recombination was highly efficient. We next isolated the tdTomato-tagged RPE cells from the RPE lineage tracer CAG-tdTomato mice. In early

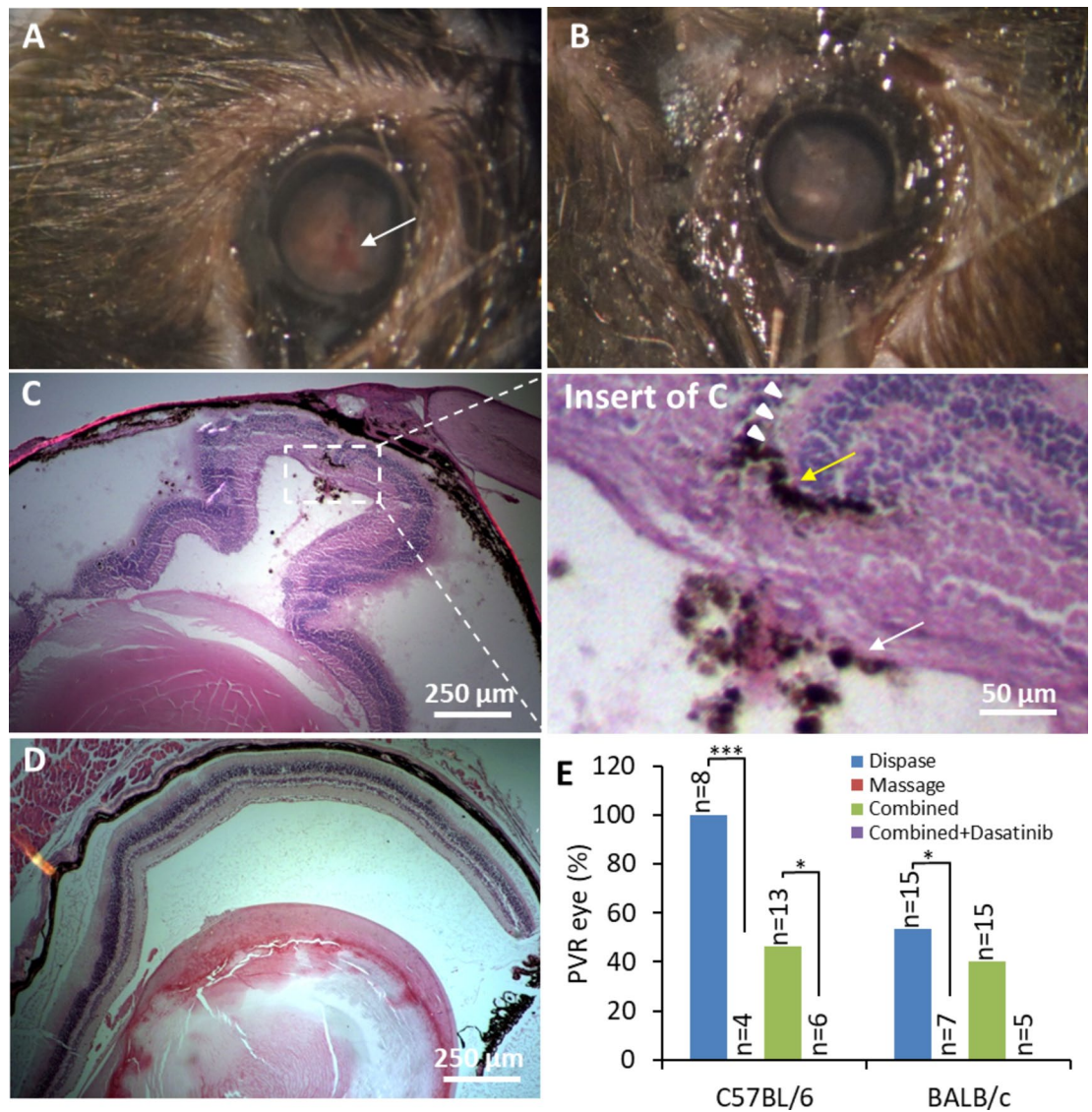


Fig. 2. Establishment of a mouse model of PVR. **A** is a massaged eye. Arrow indicates bleeding. **B** is the sham control eye. **C** is a H&E histological image of a PVR-like retina with a typical funnel-shape morphology. The yellow arrow indicates a pigmented intraretinal membrane whereas the white arrow indicates a pigmented epiretinal membrane (ERM). Arrowheads: a retinal break. **D** is a sham control retina. **E** is a bar graph depicting the efficacies of PVR-like retinas induced by 0.6 U/mL dispase, massage, and combined treatments, and effect of 0.3 μ M dasatinib treatment on reducing the PVR in two different mouse strains. *, $p \leq 0.05$; ***, $p \leq 0.001$.

primary cultures, the RPE cells retained their hexagonal shape with the intracellular pigment as well as the red fluorescence (Fig. 3D, E). However, as the RPE cells were passaged in culture, they underwent EMT and transdifferentiated from the originally pigmented epithelial cell phenotype into non-pigmented fibroblast-like cell phenotype despite their red fluorescence was sustained (Fig. 3F, G), suggesting that the RPE lineage tracer CAG-tdTomato mice are a stable and feasible model for tracking RPE cells, regardless of their in vivo or in vitro morphological and physiological status.

In situ RPE cells travel through the neuroretina and form the epiretinal membrane (ERM)

After the intravitreal dispase treatment, mouse eyes could develop a funnel-like retinal detachment and fibrotic membranes (Fig. 2C) as compared to the sham control eyes with no PVR-like phenotype (Fig. 2D). Based on cryosections, we observed that RPE cells detached from the RPE layer and became larger size and round shape (Fig. 4A). A few of the detached RPE cells re-attached on the outer side of the retina and formed a single-cell layer PVR-like membrane on the surface of the retina (Fig. 4A). Some detached RPE cells migrated through the neural retina and formed an intraretinal membrane-like band (Figs. 2C and 4B) as the structure of the retina might have been compromised by the dispase treatment. These RPE cells remained their round shape after passing through the retina (Fig. 4C). We next stained these cryosections with the myofibroblast marker smooth muscle actin alpha (SMA α) and found no such a RPE cell positive for SMA α in the intraretinal band (Fig. 4B).

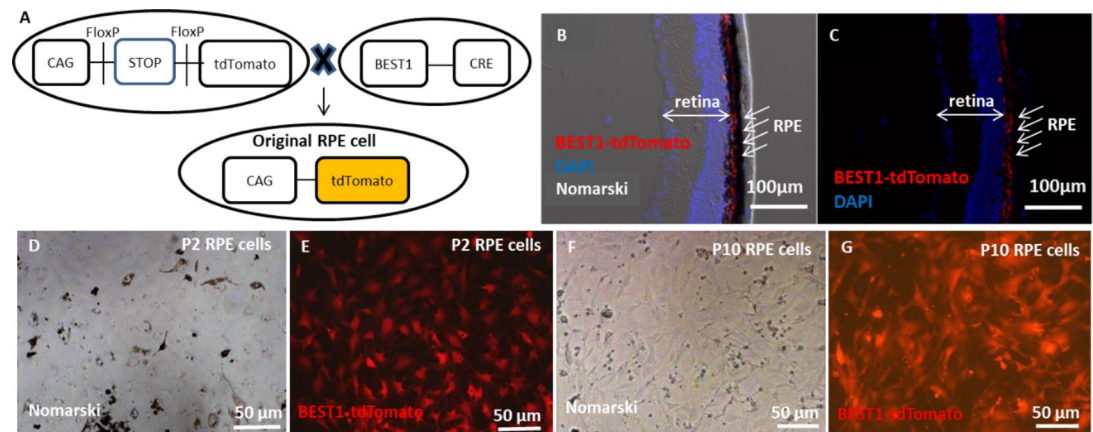


Fig. 3. Breeding for tdTomato-tagged RPE mice. **A** is a schematic diagram showing the generation of the RPE lineage tracer CAG-tdTomato mice. **B, C** Refer to the normal red fluorescent RPE layer of the RPE lineage tracer CAG-tdTomato mice. **D** and **E** refer to passage 2 (P2) whereas **F** and **G** refer to P10 primary culture of the RPE lineage tracer CAG-tdTomato mouse RPE cells.

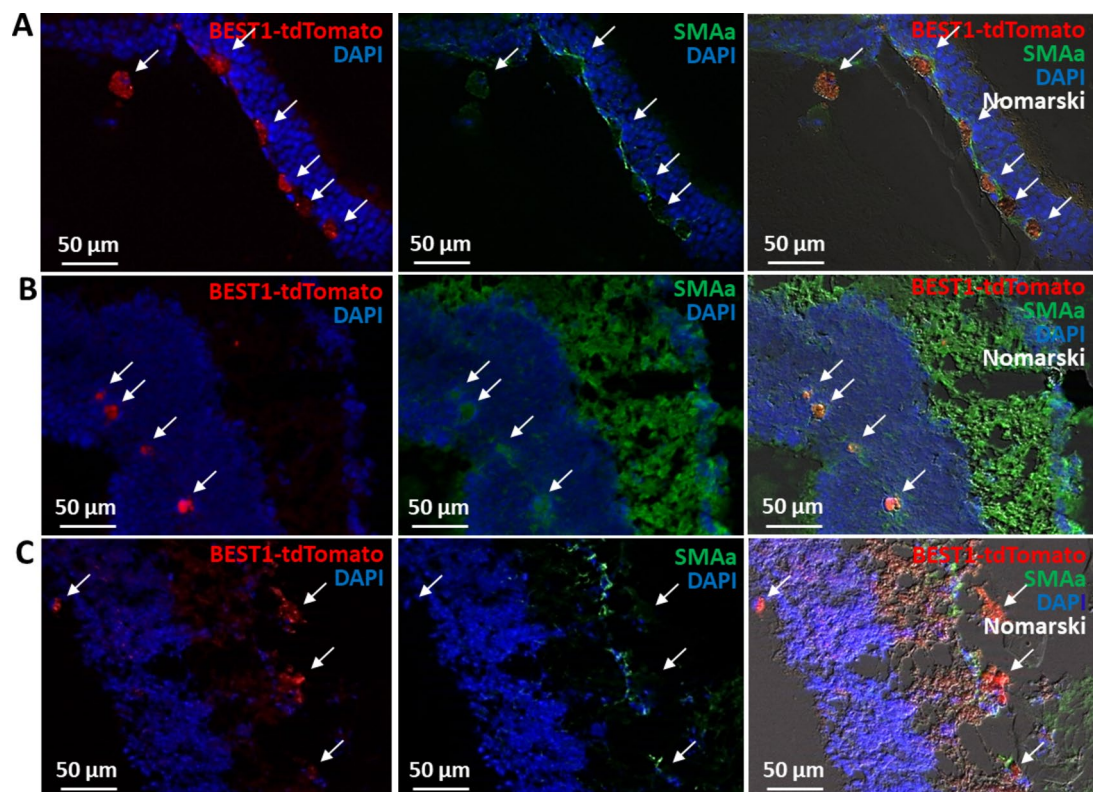


Fig. 4. The detached tdTomato-tagged RPE cells re-attached to the inner surface of the retina and travel through the intraretina to form an ERM on the outer surface of the retina. PVR-like retinal cryosections were immunostained with the antibody SMAα. **A** refers to the subretinal PVR membrane. **B** refers to the intraretinal area where the tdTomato-tagged RPE cells were migrating through the disperse-damaged retina. **C** refers the epiretinal area where the tdTomato-tagged RPE cells formed an ERM-like membrane marked by SMAα. Arrows: tdTomato-tagged RPE cells.

No RPE lineage tracer CAG-tdTomato RPE cell was detected to be for SMAα⁺ when it was in the RPE layer (data not shown), or in the retina (Fig. 4B). However, when these detached RPE cells attached to the retinal surface, regardless of the inner or outer surface of the retina, they started to express the myofibroblast marker SMAα and could form a surface PVR-like membrane on either side of the retina (Fig. 4A, C), suggesting these RPE cells might undergo EMT and gain myofibroblast properties.

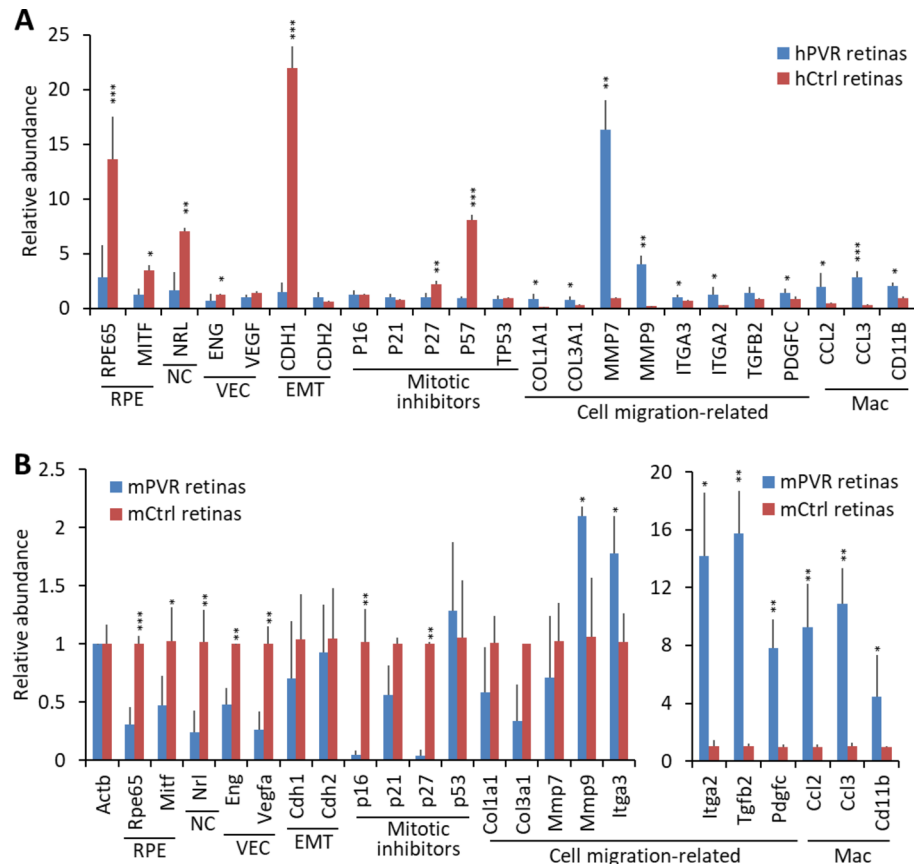


Fig. 5. Expression profiles of genes involving in PVR retinal wound healing. **A** Human PVR retinal gene expression profile (GSE41019). **B** Mouse PVR model retinal gene expression profile. *RPE* retinal pigment epithelial cell; *NC* neural cell; *VEC* vascular endothelial cell; *EMT* epithelial to mesenchymal transition; *Mac* macrophage; * $p \leq 0.05$; ** $p \leq 0.01$; *** $p \leq 0.001$. The number of retinal samples of both human and mouse is $N = 3$.

Gene expression profile of the mouse PVR model retinas resembles that of human PVR retinas

PVR is thought to be the result of abnormal retinal wound healing⁴. To clarify its underlying molecular changes over normal retinas we downloaded a set of microarray data (GSE41019) that include three human PVR retinas and three normal human retinas from the National Center for Biotechnology Information (NCBI) database. The raw intensity reads of all genes/spots were first log2 transformed and then normalized to the median values across all genes/spots and to the housekeeping gene *ACTB* values across samples following a background subtraction. Compared to the normal retinas, the PVR retinas show a downregulation of genes expressing in the RPE (e.g. *RPE65*, *MITF* and *CDH1*), the neuroretina (e.g. *NRL*), the vascular endothelium (e.g. *ENG* and *VEGF*) and inhibition of mitotic cells (e.g. *P27* and *P57*), and a upregulation of genes in cell migration (e.g. *COL1A1*, *COL3A1*, *MMP7*, *MMP9*, *ITGA2*, *ITGA3*, *TGFB2* and *PDGFC*) and immune cell infiltration (e.g. *CCL2*, *CCL3* and *CD11B*) (Fig. 5A). These gene expression profiles suggest that human PVR retinas have decreased their epithelial and endothelial cell features and increased their proliferative and mobile features, i.e., phenotypical EMT events (Fig. 5A), which seemingly are required for the PVR development.

To validate if the gene expression profile of the mouse PVR model retinas resembles the human PVR retina microarray data, we performed qPCR analyses on the retinal samples of mouse PVR model in comparison to mouse normal retina samples and found a very similar pattern (Fig. 5B) to the human's (Fig. 5A), suggesting that our mouse PVR model not only histologically and cellularly, but also molecularly resembles the human PVR retina.

Discussion

PVR as a blinding ocular complication is featured by the fibrosis on the surface of or inside the retina, resulting in fibrotic membrane formation and contraction, leading to recurrent retinal detachment⁴. The fibrotic membrane is reported to be consisted by various cell types together with an excessive deposition of the extracellular matrix (ECM)⁴. For years researchers have been trying to figure out the origin of membrane, to date the major culprit is pointed to RPE cells⁶. With surgically removed retinal membranes, the RPE cells are clearly marked out by cytokeratin 18 and RPE65 retinal flat-mount immunohistochemistry^{11,25–27}, the structure is also identified by

electron microscope²⁸. An in vitro study found that RPE cells transform their epithelial phenotype to mesenchymal phenotype to increase their proliferative ability and mobility when they have lost cell–cell contact²⁹. It is reported that only half of SMA α ⁺ myofibroblast cells in the ERMs are derived from the cytokeratin positive RPE cells¹¹. Therefore we should keep in mind that ERMs also contain other lineages like Müller and microglial cells in addition to RPE when comparing ERMs with hRPE (Fig. 1D). Besides, RPE cell is also considered as a potential stem cell for restoring retinal function²⁰. Researchers reported that under human amniotic fluid culture, the RPE cell is able to differentiate into a rod photoreceptor and ganglion neural cell³⁰. Such a multifaceted cell type could lose their original gene expression pattern and turn into other unknown expression patterns. For example, the expression of the RPE marker RPE65 decreases over culture passages. However, the expression of a cell marker is not constant and stable for tracking the origin of RPE cells during PVR pathogenesis. In contrast, our study on the genetically modified mouse RPE cells tagged with the red fluorophore tdTomato had shown the red fluorescence was not influenced by cell morphological or physiological changes after a cell identity switch of the original RPE. The red fluorophore seems to be a genetic imprinting to the starting RPE cells and exerts its tagging function in tracing the RPE origin. The tdTomato-tagged RPE cells did not decrease their fluorescence in our in vivo and in vitro studies. We showed for the first time that migrated RPE cells had gained a myofibroblast feature by expressing SMA α . It is of note that this mouse PVR model has its limitation, the origin of the excreted ECM is not traceable by adding a genetic tag to the mice although it has been suggested that the ECM proteins like collagen I and collagen II could be excreted by both RPE and Müller cells¹¹.

For PVR models, rabbits are commonly used because their lens is relatively small and they have a larger vitreous cavity comparing to rodents. However, mouse genes are more conservative and comparable to humans³¹, although its small eye with relatively large lens does not mimic the human eye structure and interferes with intraocular procedures. Many researchers had tried to induce PVR in animal experiments. For instance, injecting RPE cells into the swine and rabbit vitreous would produce abundant fibrotic membranes, the injected RPE cells would proceed EMT and mainly turn into myofibroblasts in about two weeks no matter whether the RPE cells are autologous or homologous^{18,32}. However, the procedure does not imitate the natural development of human PVR. Human PVR formation is a complicated process that involves a series of events that are not yet completely understood, animal models with intravitreal exogenous cells are unlikely recapitulate human PVR pathogenesis. Although lensectomy, vitrectomy and retinectomy are used in mice to keep constant retinal detachment for developing EMT and fibrous cellular membrane²⁴, the corneal incision is huge for lens extraction thus leads to extensive damage to the eye structure. The procedure of injecting dispase into the vitreous is relatively easier and reproducible, but a high concentration of dispase destructs the lens and retina extensively³³. Dispace was reported to induce ERMs without RPE-derived cells³⁴. We tried to scrape mouse epiretinal surface or produced bullous retinal detachment by subretinally injecting PBS, but the affected retinas healed very soon, they were flattened even in the next day (data not shown). The major reason behind the quick heal is likely that the big mouse lens can easily push the deform retina back to its normal location. Therefore, to spontaneously induce PVR by producing long term retinal detachment in mice without extensive damages or exotic cells, we injected diluted dispase to stimulate traumatic retinal detachment as dispase would keep the retina from reattachment as dispase is a protease that causes inflammation through the retina. The relatively longer period for PVR formation (7 to 8 weeks rather than 2 weeks) is more alike human PVR formation. Although dispase, unlike massage or tear to physically damage the retina, the compromised retina either physically by a surgery or enzymatically by dispase allows RPE cells depart from the retinal epithelium and migrate through the damaged retina like from a tear to potentially form ERM on the surface of the retina, mimicking partly the process of human PVR.

The EMT procession, which we expected to occur inside and outside the retina right after RPE cells lost their cell–cell contact and left the RPE layer, occurs in human ERMs (Fig. 1D) and human PVR retinas (Fig. 5A). The EMT might also occur in our mouse PVR model retinas as the RPE, neural and vascular endothelial cells appeared to loss their identify and to gain proliferative and mobile abilities based on their gene expression profiles (Fig. 5B) although two typical EMT genes (i.e., *Cdh1* and *Cdh2*) did not change their expression level accordingly (Fig. 5B). In fact, in our study we showed some RPE cells migrating to the surface of the retina with transforming into mesenchymal like cells (Fig. 4C). The RPE cell migration is not uncommon in ocular disease, such as in the development of retinal pigmentosa (RP), RPE cells invade the neuroretina and turn out to be 'bone spicule' like pigment change³⁵. We suppose that the migration might result from the microenvironmental difference between Bruch's membrane, the place where RPE cells initially stay, and the surface of the neuroretina, where RPE is exposed to the vitreous and lack of blood supply. However, what triggered the RPE to express myofibroblast marker and induced contraction of retina is still a question and needs to be investigated.

Conclusion

Our mouse PVR model not only histologically and cellularly, but molecularly resembles human PVR and is suitable for molecular mechanism and pharmaceutical studies.

Data availability

The datasets used and/or analyzed in this current study are available from the corresponding author on reasonable request.

Received: 26 July 2024; Accepted: 11 March 2025

Published online: 21 March 2025

References

1. Tseng, W., Cortez, R. T., Ramirez, G., Stinnett, S. & Jaffe, G. J. Prevalence and risk factors for proliferative vitreoretinopathy in eyes with rhegmatogenous retinal detachment but no previous vitreoretinal surgery. *Am. J. Ophthalmol.* **137**, 1105–1115. <https://doi.org/10.1016/j.ajo.2004.02.008> (2004).
2. Chaudhary, R., Dretzke, J., Scott, R., Logan, A. & Blanch, R. Clinical and surgical risk factors in the development of proliferative vitreoretinopathy following retinal detachment surgery: a systematic review protocol. *Syst. Rev.* **5**, 107. <https://doi.org/10.1186/s13643-016-0284-7> (2016).
3. Kwon, O. W., Song, J. H. & Roh, M. I. Retinal detachment and proliferative vitreoretinopathy. *Dev. Ophthalmol.* **55**, 154–162. <https://doi.org/10.1159/000438972> (2016).
4. Idrees, S., Sridhar, J. & Kuriyan, A. E. Proliferative vitreoretinopathy: A review. *Int. Ophthalmol. Clin.* **59**, 221–240. <https://doi.org/10.1097/IIO.0000000000000258> (2019).
5. The classification of. Retinal detachment with proliferative vitreoretinopathy. *Ophthalmology* **90**, 121–125 (1983).
6. Pastor, J. C. et al. Proliferative vitreoretinopathy: A new concept of disease pathogenesis and practical consequences. *Prog. Retin. Eye Res.* **51**, 125–155. <https://doi.org/10.1016/j.preteyeres.2015.07.005> (2016).
7. Zhao, H. M., Sheng, M. J. & Yu, J. Expression of IGFBP-6 in a proliferative vitreoretinopathy rat model and its effects on retinal pigment epithelial cell proliferation and migration. *Int. J. Ophthalmol.* **7**, 27–33. <https://doi.org/10.3980/j.issn.2222-3959.2014.01.05> (2014).
8. Chiba, C. The retinal pigment epithelium: an important player of retinal disorders and regeneration. *Exp. Eye Res.* **123**, 107–114. <https://doi.org/10.1016/j.exer.2013.07.009> (2014).
9. Guidry, C. The role of Muller cells in fibrocontractive retinal disorders. *Prog. Retin. Eye Res.* **24**, 75–86. <https://doi.org/10.1016/j.preteyeres.2004.07.001> (2005).
10. Fischer, A. J., Zelinka, C. & Milani-Nejad, N. Reactive retinal microglia, neuronal survival, and the formation of retinal folds and detachments. *Glia* **63**, 313–327. <https://doi.org/10.1002/glia.22752> (2015).
11. Feist, R. M. Jr., King, J. L., Morris, R., Witherspoon, C. D. & Guidry, C. Myofibroblast and extracellular matrix origins in proliferative vitreoretinopathy. *Graefes Archive Clin. Experimental Ophthalmol.* = *Albrecht Von Graefes Archiv fur Klinische Und Experimentelle Ophthalmologie*. **252**, 347–357. <https://doi.org/10.1007/s00417-013-2531-0> (2014).
12. Tamiya, S. & Kaplan, H. J. Role of epithelial-mesenchymal transition in proliferative vitreoretinopathy. *Exp. Eye Res.* **142**, 26–31. <https://doi.org/10.1016/j.exer.2015.02.008> (2016).
13. Saika, S. et al. Epithelial-mesenchymal transition as a therapeutic target for prevention of ocular tissue fibrosis. *Endocr. Metab. Immune Disord. Drug Targets*. **8**, 69–76 (2008).
14. Bu, S. C., Kuijer, R., Li, X. R. & Hooymans, J. M. Los, L. I. Idiopathic epiretinal membrane. *Retina* **34**, 2317–2335. <https://doi.org/10.1097/IAE.0000000000000349> (2014).
15. Chen, S. H. et al. Doxycycline ameliorates the severity of experimental proliferative vitreoretinopathy in mice. *Int. J. Mol. Sci.* **22**. <https://doi.org/10.3390/ijms222111670> (2021).
16. Zhang, L. et al. Antisense oligonucleotide targeting c-fos mRNA limits retinal pigment epithelial cell proliferation: a key step in the progression of proliferative vitreoretinopathy. *Exp. Eye Res.* **83**, 1405–1411. <https://doi.org/10.1016/j.exer.2006.07.020> (2006).
17. Heffer, A. et al. A mouse model of proliferative vitreoretinopathy induced by intravitreal injection of gas and RPE cells. *Transl. Vis. Sci. Technol.* **9**. <https://doi.org/10.1167/tvst.9.7.9> (2020).
18. Agrawal, R. N. et al. In vivo models of proliferative vitreoretinopathy. *Nat. Protoc.* **2**, 67–77. <https://doi.org/10.1038/nprot.2007.4> (2007).
19. Umazume, K. et al. Inhibition of PVR with a tyrosine kinase inhibitor, Dasatinib, in the swine. *Invest. Ophthalmol. Vis. Sci.* **54**, 1150–1159. <https://doi.org/10.1167/iovs.12-10418> (2013).
20. Chen, F. et al. Sphere-induced reprogramming of RPE cells into dual-potential RPE stem-like cells. *EBioMedicine* **52**, 102618. <https://doi.org/10.1016/j.ebiom.2019.102618> (2020).
21. Sanchez-Tillo, E. et al. EMT-activating transcription factors in cancer: beyond EMT and tumor invasiveness. *Cell. Mol. Life Sci.* **69**, 3429–3456. <https://doi.org/10.1007/s00018-012-1122-2> (2012).
22. Datilbagi, A. et al. Experimental models to study Epithelial-Mesenchymal transition in proliferative vitreoretinopathy. *Int. J. Mol. Sci.* **24**. <https://doi.org/10.3390/ijms24054509> (2023).
23. Han, H. et al. Activated blood coagulation factor X (FXa) contributes to the development of traumatic PVR through promoting RPE Epithelial-Mesenchymal transition. *Invest. Ophthalmol. Vis. Sci.* **62**, 29. <https://doi.org/10.1167/iovs.62.9.29> (2021).
24. Saika, S. et al. Smad3 is required for dedifferentiation of retinal pigment epithelium following retinal detachment in mice. *Lab. Invest.* **84**, 1245–1258. <https://doi.org/10.1038/labinvest.3700156> (2004).
25. Hiscott, P. S., Grierson, I. & McLeod, D. Retinal pigment epithelial cells in epiretinal membranes: an immunohistochemical study. *Br. J. Ophthalmol.* **68**, 708–715 (1984).
26. Fernandez-Bueno, I. et al. Histology and immunochemistry evaluation of autologous translocation of retinal pigment epithelium-choroid graft in Porcine eyes. *Acta Ophthalmol.* **91**, e125–132. <https://doi.org/10.1111/aos.12001> (2013).
27. Zheng, X. Z., Du, L. F. & Wang, H. P. An immunohistochemical analysis of a rat model of proliferative vitreoretinopathy and a comparison of the expression of TGF-beta and PDGF among the induction methods. *Bosnian J. Basic. Med. Sci. / Udruzenje Basic. ih Medicinskih znanosti = Association Basic. Med. Sci.* **10**, 204–209 (2010).
28. Yeo, J. H., Sadeghi, J., Campochiaro, P. A., Green, W. R. & Glaser, B. M. Intravitreal fibronectin and platelet-derived growth factor. New model for traction retinal detachment. *Arch. Ophthalmol.* **104**, 417–421 (1986).
29. Tamiya, S., Liu, L. & Kaplan, H. J. Epithelial-mesenchymal transition and proliferation of retinal pigment epithelial cells initiated upon loss of cell-cell contact. *Investig. Ophthalmol. Vis. Sci.* **51**, 2755–2763. <https://doi.org/10.1167/iovs.09-4725> (2010).
30. Ghaderi, S. et al. Human amniotic fluid promotes retinal pigmented epithelial cells' trans-differentiation into rod photoreceptors and retinal ganglion cells. *Stem. Cells. Dev.* **20**, 1615–1625. <https://doi.org/10.1089/scd.2010.0390> (2011).
31. Miller, W., Makova, K. D., Nekrutenko, A. & Hardison, R. C. Comparative genomics. *Annu. Rev. Genom. Hum. Genet.* **5**, 15–56. <https://doi.org/10.1146/annurev.genom.5.061903.180057> (2004).
32. Umazume, K. et al. Proliferative vitreoretinopathy in the Swine-a new model. *Investig. Ophthalmol. Vis. Sci.* **53**, 4910–4916. <https://doi.org/10.1167/iovs.12-9768> (2012).
33. Tan, J., Liu, Y., Li, W. & Gao, Q. Ocular pathogenesis and immune reaction after intravitreal disperse injection in mice. *Mol. Vis.* **18**, 887–900 (2012).
34. Canto Soler, M. V., Gallo, J. E., Dodds, R. A. & Suburo, A. M. A mouse model of proliferative vitreoretinopathy induced by disperse. *Exp. Eye Res.* **75**, 491–504. <https://doi.org/10.1006/exer.2002.2031> (2002).
35. Jones, B. W. et al. Retinal remodeling in human retinitis pigmentosa. *Exp. Eye Res.* <https://doi.org/10.1016/j.exer.2016.03.018> (2016).

Acknowledgements

None.

Author contributions

YC and XL performed the experiments, collected, and analyzed the data, and wrote the manuscript. AK, XL, LG and JYL assisted the experimental performance. HJK participated in the experimental design. YL and DCD designed experiments, analyzed the data, and wrote the manuscript. All authors read and approved the final manuscript.

Declarations

Competing interests

The authors declare no competing interests.

Additional information

Supplementary Information The online version contains supplementary material available at <https://doi.org/10.1038/s41598-025-93999-y>.

Correspondence and requests for materials should be addressed to D.C.D. or Y.L.

Reprints and permissions information is available at www.nature.com/reprints.

Publisher's note Springer Nature remains neutral with regard to jurisdictional claims in published maps and institutional affiliations.

Open Access This article is licensed under a Creative Commons Attribution-NonCommercial-NoDerivatives 4.0 International License, which permits any non-commercial use, sharing, distribution and reproduction in any medium or format, as long as you give appropriate credit to the original author(s) and the source, provide a link to the Creative Commons licence, and indicate if you modified the licensed material. You do not have permission under this licence to share adapted material derived from this article or parts of it. The images or other third party material in this article are included in the article's Creative Commons licence, unless indicated otherwise in a credit line to the material. If material is not included in the article's Creative Commons licence and your intended use is not permitted by statutory regulation or exceeds the permitted use, you will need to obtain permission directly from the copyright holder. To view a copy of this licence, visit <http://creativecommons.org/licenses/by-nc-nd/4.0/>.

© The Author(s) 2025